6. Stress Field at Yucca Mountain, Nevada

By Joann M. Stock *and* John H. Healy

CONTENTS

Abstract

Hydraulic fracturing stress measurements performed in four holes (USW G–1, USW G–2, USW G–3, and Ue25P1) indicate that at Yucca Mountain, the least horizontal stress S_h is less than the vertical stress S_v. Values of the greatest horizontal stress S_H are intermediate between S_h and S_v, corresponding to a normal faulting regime with values of $\phi = (S_H - S_h)/(S_v - S_h)$ between 0.25 and 0.7. Drilling-induced hydraulic fractures seen on borehole televiewer logs indicate an S_h direction of N. 60° W. to N. 65° W. in USW G–1, USW G–2, and USW G–3. The same S_h direction is inferred from breakout orientations in USW G–2 and Ue25P1. The S_h values in the upper parts of the three USW G holes are less than the pressure of a column of water filling the borehole to the surface. Thus, the long drilling-induced hydraulic fractures in the shallow parts of these holes could have been formed in attempts to maintain circulation during drilling. These low S_h values may be intimately related to the low water table and fracture-dominated hydrology of Yucca Mountain.

INTRODUCTION

Information on the state of stress at Yucca Mountain is important to the evaluation of its suitability as a site for a high-level radioactive waste repository. A knowledge of the stress field is a key parameter in our understanding of the tectonic setting of the site, and the evaluation of possible failure behavior of preexisting faults. This knowledge permits estimation of the additional stresses which may be induced by the repository, for instance, due to excavation or thermal effects of the waste. Because the magnitudes of the principal stresses influence fluid transport through fractures, the stress field may be intimately related to the hydrologic regime present at Yucca Mountain.

The hydraulic fracturing stress measurements performed at Yucca Mountain, as part of the Nevada Nuclear Waste Storage Investigations program of the U.S. Department of Energy, yield information on the directions and magnitudes of the principal stresses at the locations of the individual tests, made within holes USW G–1, USW G–2, USW G–3, and Ue25P1 (fig. 6.1). When collectively evaluated and combined with other stress field indicators, the results provide an important basis for more detailed studies, with specific reference to the depths being considered for the repository facility.

Acknowledgments

We thank W.F. Brace, Art McGarr, and Mary Lou Zoback for helpful comments. Hans Swolfs' suggestions were also much appreciated, although he does not endorse all of our conclusions. The field measurements were performed in cooperation with the Nevada Operations Office of the U.S. Department of Energy under interagency agreement DE–AI08–78ET44802. J.M. Stock thanks the Fannie and John Hertz Foundation for supporting her graduate work at the Massachusetts Institute of Technology, during which time this paper was completed.

STRESS MAGNITUDES

The hydraulic fracturing method directly measures the magnitude of the least horizontal principal stress, S_h, and indirectly yields an estimate of the value of the greatest horizontal principal stress, S_H. The method, first proposed by Hubbert and Willis (1957), is now fairly standard and is described in detail elsewhere (see Hickman and Zoback, 1983). Our test procedures and equipment setup are described in more detail by Healy and others (1984) and Stock and others (1984, 1986).

This method is based on an analytic solution for stress around a cylindrical hole in an elastic, isotropic medium (Hubbert and Willis, 1957). If S_h and S_H are perpendicular to the borehole axis, the minimum compressive stress tangential to the borehole occurs at the azimuth of S_H. Therefore, when the pressure in the holes exceeds this minimum stress, a hydraulic fracture should be formed at this azimuth and propagate perpendicularly to the direction of S_h. The S_h is obtained by observing the normal stress across the newly created hydrofracture, defined as the pressure at which the fracture closes, or the ISIP (instantaneous shut in pressure)

visible on the pressure-time curves. The S_H is calculated from the fracture reopening pressure on the second cycle, according to the method of Bredehoeft and others (1976). The pore pressure, which is needed for the S_H calculation, is calculated as the hydrostatic pressure from the observed water level in the hole. If testing has altered the pore pressure, so that its value is uncertain, then S_H cannot be well constrained. Because this was the case in many of our tests, few credible S_H values were obtained.

The third principal stress must be vertical, and is calculated by integrating the weight of the overlying rocks, obtained from compensated density logs and (or) borehole gravimetry. The compensated density logs, gravimetry (where available), and density measurements of core samples were generally in close agreement for these four holes, so most of the estimates of vertical stress magnitudes are likely to be quite accurate. Where the hole has a large component of drift, such as in the lower part of USW G–3, corrections

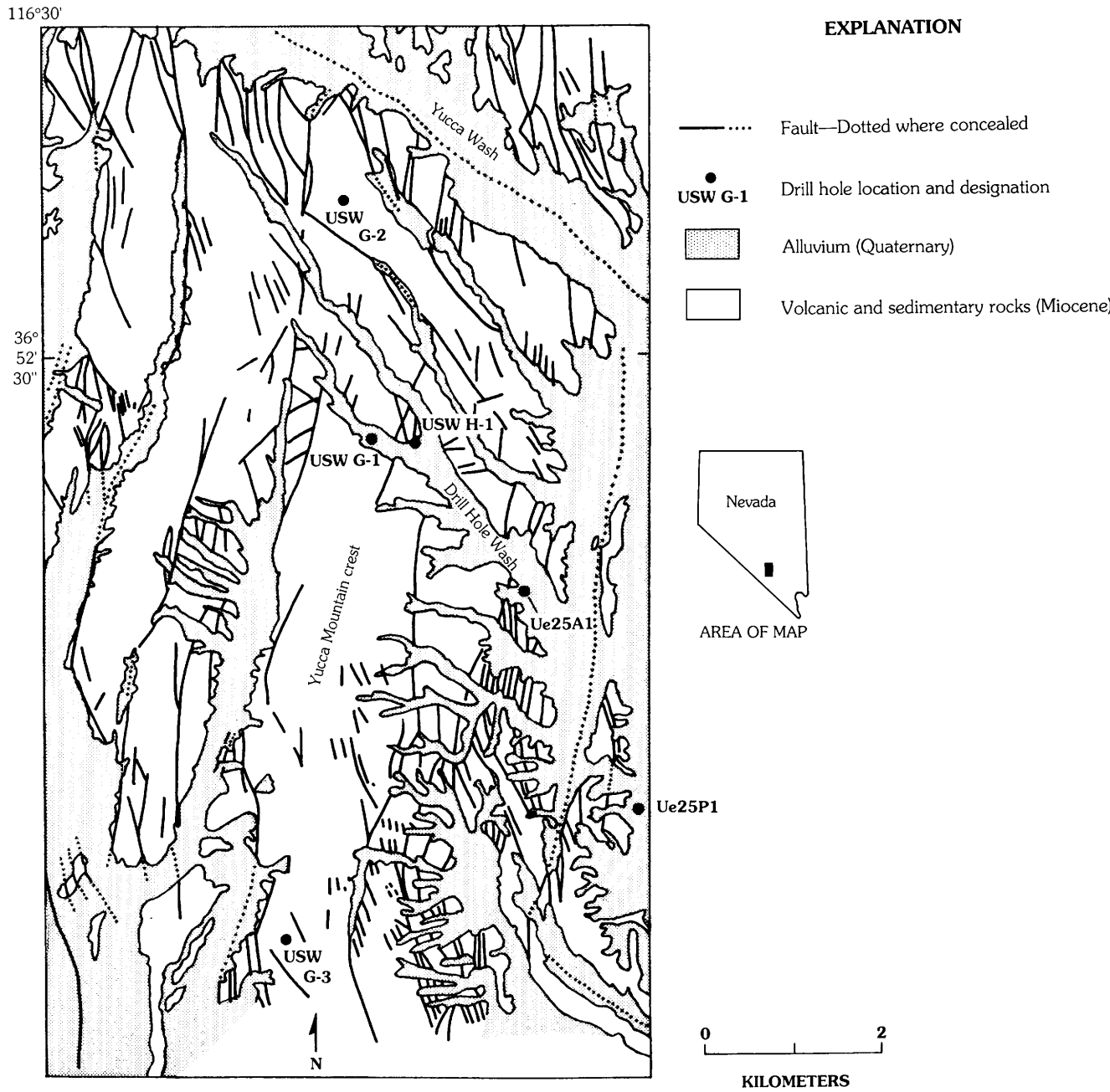

Figure 6.1. Generalized geologic map of Yucca Mountain, Nev., showing locations and names of drill holes discussed in text. Geology generalized from Scott and Bonk (1984).

must be made for absolute depth and changes in overburden due to rapidly varying surface topography, thus adding uncertainty to the estimate of S_v.

If the topography is irregular, small-wavelength variations should be averaged out before calculation of S_v at depth. Such corrections are most important for USW G-3. For instance, the elevation of the surface at USW G-3 is 1,480 m; however, the average surface elevation within a circle of 700 m radius centered on the top of the hole is approximately 1,390 m. If the circle is centered on the surface projection of the position of our lowest test, the average surface elevation is 1,370 m. The S_v values listed for the USW G-3 tests (table 6.1) include a correction obtained using a 700-m radius because that is the average depth of the USW G-3 tests below the surface. Maximum uncertainty limits on these values can be estimated using the uncorrected value of S_v as an upper bound, and the average topography in the absence of the excess height of the ridge as a lower bound; this gives an uncertainty of $\pm$2.0–2.5 MPa for the S_v values in USW G-3. An estimate for the S_v correction can also be derived analytically if the surface topography can be approximated as a smooth function, and density and elastic constants are assumed uniform (see Swolfs and Savage, 1985).

Stress values obtained at Yucca Mountain are summarized in table 6.1 and figure 6.2. The corresponding pressure-time data have been discussed elsewhere (Healy and others, 1984; Stock and others, 1984, 1986). We reproduce here some sample test curves (fig. 6.3) to illustrate the details of interpretation and some unusual conditions encountered in the Yucca Mountain holes.

For the deeper successful tests in these holes, the breakdown pressures were clear and distinct, and the ISIPs occurred at pressures higher than the surface hydrostat (pressure of a column of water filling the hole to the surface). The pressure-time curves show an inflection when the pressure equals the surface hydrostat, at a level below the S_h value obtained from ISIP and steprate injection tests on the final cycles. Such behavior was seen during the tests at 1,038, 1,218, and 1,288 m in USW G-1; 1,026 and 1,209 m in USW G-2; and 1,573 m in Ue25P1 (see fig. 6.3*A*).

On some other tests, good breakdown pressures were observed, with ISIP values less than the surface hydrostat. Such behavior was seen during the three successful tests in USW G-3, at 1,074, 1,338, and 1,356 m; and in USW G-1, at 646, 792, and 945 m (see fig. 6.3*B*).

Several tests showed breakdown pressures that were equal to the fracture reopening pressure on later cycles. This suggested that the effective tensile strength of the formation was zero, probably because a preexisting fracture was present in the interval and was reopened during the test. As this occurred in regions of the hole where preexisting fractures are likely (above the water table in USW G-2 and in bedded carbonate units at 1,564 and 1,693 m in Ue25P1), we prefer this explanation for the repeatable character of these test curves (see fig. 6.3*C*). Preexisting fractures may not be oriented perpendicularly to the S_h direction; thus, the estimated normal stress across them can only be used as an upper bound on the value of the minimum stress (in this case, S_h) at depth.

The types of pressure-time curves discussed above encompass those from which values of S_h or S_H were obtained. A fourth type of curve showed a large pressure drop once the interval was open to the pressure in the tubing string. This behavior may be due to an unidentified equip-

Table 6.1. Summary of hydraulic fracturing stress measurements at Yucca Mountain
[Pore pressures are based on the water levels recorded before testing: USW G-1, 575 m; USW G-2, 526 m; USW G-3, 752 m; Ue25P1, 385 m]

Drill hole	Logged depth (m)	True depth (m)	S_v (MPa)	S_h (MPa)	S_H (MPa)	Pore pressure (MPa)	ϕ
USW G-2-----	295	295	6.1	$\leq$ 5.1±0.1	--	0	--
USW G-2-----	418	418	8.4	$\leq$ 5.4±0.1	--	0	--
USW G-2-----	432	432	8.7	$\leq$ 5.5±0.1	--	0	--
USW G-1-----	646	646	12.9	4.2±0.2	--	0.7	--
USW G-1-----	792	792	15.9	7.2±0.2	--	2.2	--
USW G-1-----	945	945	19.2	9.0±0.2	--	3.6	--
USW G-3-----	1,074	[1]1,068	20.6±2.0	6.8±0.2	10.7±1.0	3.1	~0.28
USW G-2-----	1,026	1,026	20.8	11.1±0.2	16.8±0.4	4.9	.59
USW G-1-----	1,038	1,038	21.4	10.6±0.2	--	4.5	--
USW G-1-----	1,218	1,218	25.5	12.1±0.2	--	6.3	--
USW G-2-----	1,209	1,209	25.5	12.0±0.2	17.3±0.4	6.7	.39
USW G-3-----	1,338	[1]1,321	25.8±2.5	11.5±0.2	17.5±0.9	5.6	~.45
USW G-3-----	1,356	[1]1,338	26.3±2.5	11.4±0.2	18.1±0.8	5.7	~.45
USW G-1-----	1,288	1,288	27.2	14.8±0.2	17.9	7.0	.25
Ue25P1------	1,564	1,564	35.3	$\leq$33.7±0.2	--	11.5	--
Ue25P1------	1,573	1,573	35.6	20.7±0.2	31.0±1.1	11.6	.69
Ue25P1------	1,693	1,693	38.8	$\leq$36.5±1.0	--	12.8	--

[1] Depths in USW G-3 were corrected to true depth prior to calculation of pore pressure and S_H. S_v values in USW G-3 have been corrected for average elevation and are therefore approximate.

ment problem or to some unusual property of the rock in the test interval. Such behavior was common in tests in the tuffs and lavas of the Calico Hills unit in USW G-2.

STRESS DIRECTIONS

The orientations of the principal stresses can be found from observation of directional features in drill holes, including hydraulic fractures (both test-induced and drilling-induced) and directional wellbore spalling, or breakouts. These and other borehole features are visible on acoustic televiewer logs of the drill holes. Operational principles of the televiewer have been described by Zemanek and others (1969), and details of interpretation of borehole features are described in our previous reports.

Preexisting fractures intersected by the borehole can be seen as dark, sinusoidal traces in the televiewer log. Their amplitude and phase can be measured to determine the strike and dip of the fracture. Such fractures are present in all four holes. Their strike directions tend to vary from north to northeast, they dip steeply, and they tend to become less steep, with more scattered orientations, at depth. Their orientations provide no direct indication of stress direction, but they do show that the degree of fracture anisotropy, which may be pronounced at shallow levels, decreases or disappears at depth.

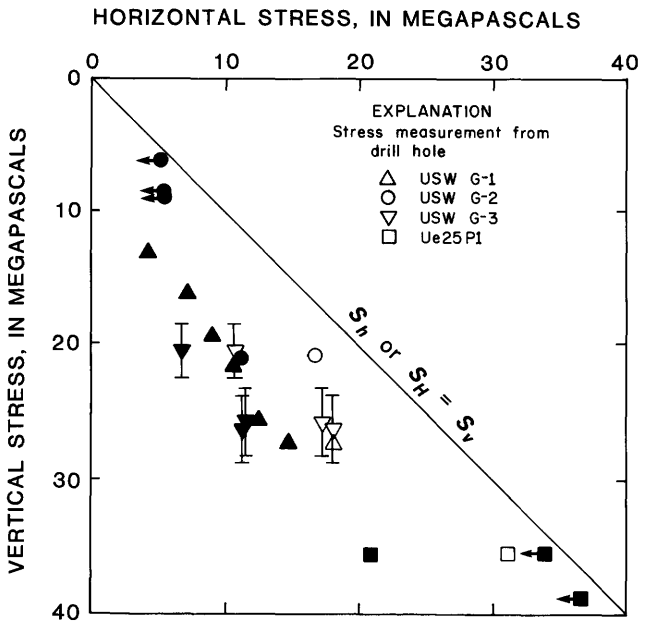

Figure 6.2. Values of least horizontal principal stress S_h (solid symbols) and greatest horizontal principal stress S_H (open symbols) plotted as a function of vertical stress, S_v. Horizontal arrows indicate that values are upper bounds. Vertical bars indicate range of uncertainty associated with S_v values in drill hole USW G-3, due to topographic effects.

In addition to preexisting fractures, very steep to vertical fractures follow the hole for many tens of meters in the televiewer logs of USW G-1 (520–760 m depth), USW G-2 (526–678 m depth), and USW G-3 (at intervals from 882 to 1,018 m). In some cases these do not appear to be throughgoing fractures, as they have no observed trace on the opposite azimuth in the televiewer log. They vary in aspect from en echelon and jagged, connected to or interrupted by throughgoing fractures, to straight and continuous. These fractures have an average strike of N. 25° E. in USW G-3, N. 15° E.-N. 35° E. in USW G-1, and N. 25° E.-N. 30° E. in USW G-2. Most notably, these fractures cannot be identified on corresponding sections of the drill core, suggesting that they were formed after coring but prior to the collection of the televiewer data. We believe that these are hydraulic fractures induced by drilling. The low values of S_h measured elsewhere in the holes, if present at the depths of these features, could have been exceeded by raising the water level to the surface by filling the hole with fluid. Such fractures could accept fluid when the water level was still below the surface of the hole, providing a reasonable

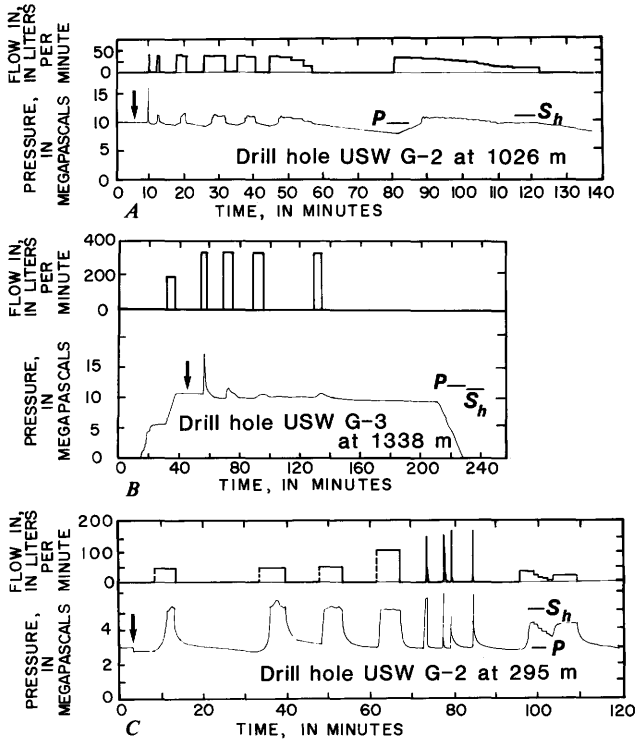

Figure 6.3. Pressure-time curves from hydraulic fracturing tests at Yucca Mountain. Least horizontal principal stress (instantaneous shut-in pressure), S_h; surface hydrostatic pressure, *P*. *A*, Clear breakdown with S_h greater than *P*. *B*, Clear breakdown with S_h less than *P*. *C*, Breakdown pressure equal to fracture reopening pressure on later cycles, indicating that a preexisting fracture is being reopened. Arrows show time at which test interval was opened to pressure in tubing string.

explanation for the huge volumes of drilling fluid that were lost in the three holes and the continuous loss of circulation during drilling. In Ue25P1, drilling-induced hydraulic fractures are not observed, and circulation was maintained during drilling.

If these are indeed hydraulic fractures, their strike implies an S_h direction of N. 60° W.-N. 65° W. in these three holes. This direction is also suggested by the orientations of breakouts in USW G-1, USW G-2, and Ue25P1. These breakouts are spalled portions of the borehole wall which are visible as dark bands of the televiewer log at azimuths 180° apart. When the returning televiewer signal is plotted as traveltime against azimuth, to yield a cross section of the shape of the hole, these dark patches are seen to correspond to sections of the hole with unusually large radii.

Breakouts in many regions provide consistent, regional information on the horizontal principal stress directions because they form at the azimuth of the maximum compressive stress around the borehole, the S_H azimuth (see Bell and Gough, 1983). The average N. 60° W. to N. 65° W. orientation of breakouts in USW G-2 (between 1,053 and 1,219 m) and N. 60° W. azimuth of breakouts in Ue25P1 (between 1,524 and 1,676 m) suggest an S_h orientation of N. 60° W., consistent with the orientation inferred from the drilling-induced hydraulic fractures. Breakouts from 1,113 to 1,202 m in USW G-1 had a S. 80° W. azimuth, indicating an S_h direction 40° off from all other directional data. These occur in an inclined portion of the hole (9° from vertical); however, modeling shows that this breakout azimuth could not have resulted from the observed hole deviation and the measured Yucca Mountain stress field with S_H at N. 25° E., S_h at N. 65° W., S_v vertical, and ϕ, or $(S_H-S_h)/(S_v-S_h)$, between 0.25 and 0.7 (Stock and others, 1985). Therefore, a local perturbation of the stress field seems likely.

AGREEMENT WITH REGIONAL DATA

The observed stress directions are in good agreement with directions derived from regional data showing northwest to west-northwest orientation of S_h (Carr, 1974; Zoback and Zoback, 1980; Stock and others, 1985). The N. 60° W. to N. 65° W. S_h direction that we find at Yucca Mountain is slightly more westerly than the N. 45° W. to N. 55° W. S_h orientations reported from hydraulic fracturing in Rainier Mesa (Haimson and others, 1974; Warren and Smith, 1985) and the N. 45° W. to N. 60° W. S_h orientation derived from breakouts in drill holes in Yucca Flat and Pahute Mesa (Carr, 1974; Springer and Thorpe, 1981). However, they are within the scatter of this regional data and are considered to be consistent with it.

The observed stress magnitudes indicate a normal faulting stress regime, with $S_h<S_H<S_v$. This is consistent with regional earthquake and geologic data, which show a combination of normal and strike-slip faulting, implying that $S_h<S_H<S_v$ (see Stock and others, 1985). The ratio ϕ, equal to $(S_H-S_h)/(S_v-S_h)$ in a normal faulting regime, indicates how close the stress magnitudes lie to a "pure normal faulting regime" ($\phi=0$) or a "combined normal and strike-slip faulting regime" ($\phi=1$). The ϕ values obtained from these holes are scattered, ranging from 0.69 (at 1,573 m in Ue25P1) to 0.25 (1,288 m in USW G-1), but the highest ϕ values are found at the deepest structural levels. If the Yucca Mountain stress field tends toward higher values with structural depth, extrapolation to deeper levels should be based on higher ϕ values than the average of our test measurements. These may also be more representative of the regional stress field.

TOPOGRAPHIC EFFECTS ON THE HORIZONTAL STRESS

Topographic corrections to S_v are important in USW G-3, as previously noted. Analytical solutions (Savage and Swolfs, 1986) and approximations to the stress field in regions of moderate relief (McTigue and Mei, 1981) indicate that the topographic effect on the horizontal stresses is generally negligible at depths greater than one wavelength of the topography (see Jaeger and Cook, 1979, p. 373). The topographic variation at USW G-1, USW G-2, and Ue25P1 has a wavelength of 500 m; its amplitude is small, and the surface elevations of the holes are quite close to the average elevation over distances equal to the depths of our tests. Therefore, the topographic effects on S_h and S_H should be minimal. Although USW G-3 is in an area of steeper topography, modeling by Swolfs and Savage (1985) shows that the topographic effect on the horizontal stresses will be larger than the uncertainty in the hydrofrac tests only within a few hundred meters of the surface. Since our tests here were at much deeper levels, we conclude that topographic influence on the measured S_h values is too small to be detected.

Additional evidence for this conclusion comes from the S_h orientations in these holes. They all show a consistent S_h azimuth of N. 60° W. to N. 65° W., which is maintained in the presence of both a north-south topographic grain (near USW G-3 and Ue25P1) and a northwest-southeast topographic grain (near USW G-1 and USW G-2). Since a topographically controlled stress field should have S_h directions perpendicular to the strike of the topography, it appears that the Yucca Mountain stress field, at the depths studied (below the water table), is not strongly influenced by topography. The continuity of stress directions from the volcanics into the underlying carbonate rocks argues against a strong component of residual or cooling stresses influencing the stress field in the volcanic rocks, suggesting that the stress field is primarily the result of current tectonic processes.

TECTONIC IMPLICATIONS

The most important characteristic of these stress measurements is the consistently low value of S_h relative to S_v. As discussed in previous reports (Healy and others, 1984; Stock and others, 1984, 1985), the measured S_h values fall close to the limits at which frictional sliding, in a normal-faulting sense, might be expected to occur on optimally oriented preexisting faults. These low S_h values have an even more dramatic consequence: the long drilling-induced hydraulic fractures present in the upper parts of the three USW G holes. Such fractures could propagate even in the absence of a drill hole to concentrate the stresses, if the pore pressure in small cracks locally exceeded S_h. (This situation has been observed in other active extensional areas; see Zoback and Healy, 1984.)

Our data suggest that in the presence of such a stress field, if the pore pressure were to increase and exceeded S_h (due to a natural rise of the water table or to human activities, such as fluid injection), cracks could open perpendicular to S_h. These open cracks could then act as pathways for fluid flow and dissipate the excess pore pressure, until it dropped back to the S_h magnitude and the cracks could close. This implies that there may be a delicate balance between the hydrology and the stress field at Yucca Mountain, with the magnitude of S_h acting as a limit to possible increases in water level. Because S_h increases faster with depth than does the hydrostatic pressure, this effect becomes less important with depth, and is unlikely to be of concern where S_h exceeds the surface hydrostat. However, within the first kilometer of the surface, this effect is likely to be a major control on the hydrology of Yucca Mountain, and influence the tectonic response to human activities which produce major changes in local pore pressure.

CONCLUSIONS

In hydraulic fracturing stress measurements in four holes at Yucca Mountain, both the least horizontal principal stress S_h and the greatest horizontal principal stress S_H are less than the vertical stress S_v, indicating a normal-faulting stress regime. Plots of S_h and S_H as a function of S_v demonstrate that all of the S_h values are reasonably linear with respect to S_v. The few S_H values obtained from the USW holes are substantially less than S_v, whereas the one S_H value from Ue25P1 is closer to, although less than, S_v. The S_h direction is N. 60° W. to N. 65° W., in good agreement with regional stress indicators.

Upward extrapolation of these results should be done with caution, as topographic effects are more important near the surface. In order to obtain an accurate picture of the stress field in the unsaturated zone, in the area of the proposed repository, a numerical model incorporating these results and including actual topography, observed distribution and physical constants of volcanic units, and reasonable boundary conditions should be developed. Such a model should be checked for consistency with future stress measurements (hydraulic fracturing and overcoring) made closer to the position of the proposed repository, in both the saturated and unsaturated zones.

REFERENCES CITED

Bell, J.S., and Gough, D.I., 1983, The use of borehole breakouts in the study of crustal stress, *in* Zoback, M.D., and Haimson, B.C., eds., Hydraulic fracturing stress measurements: Washington, D.C., National Academy Press, p. 201–209.

Bredehoeft, J.D., Wolff, R.G., Keys, W.S., and Shuter, E., 1976, Hydraulic fracturing to determine the regional in-situ stress field, Piceance Basin, Colorado: Geological Society of America Bulletin, v. 87, p. 250–258.

Carr, W.J., 1974, Summary of tectonic and structural evidence for stress orientation at the Nevada Test Site: U.S. Geological Survey Open-File Report 74–176, 53 p.

Haimson, B.C., Lacomb, J., Jones, A.H., and Green, S.J., 1974, Deep stress measurements in tuff at the Nevada Test Site, *in* Advances in rock mechanics: Washington, D.C., National Academy of Sciences, p. 557–561.

Healy, J.H., Hickman, S.H., Zoback, M.D., and Ellis, W.L., 1984, Report on televiewer log and stress measurements in core hole USW G-1, Nevada Test Site: U.S. Geological Survey Open-File Report 84–15, 47 p.

Hickman, S.H., and Zoback, M.D., 1983, The interpretation of hydraulic fracturing pressure-time data for in-situ stress determination, *in* Zoback, M.D., and Haimson, B.C., eds., Hydraulic fracturing stress measurements: Washington, D.C., National Academy Press, p. 44–54.

Hubbert, M.K., and Willis, D.G., 1957, Mechanics of hydraulic fracturing: Journal of Petroleum Technology, v. 9, p. 153–168.

Jaeger, J.C., and Cook, N.G.W., 1979, Fundamentals of rock mechanics, 3d ed.: London, Chapman and Hall, 593 p.

McTigue, D.F., and Mei, C.C., 1981, Gravity-induced stresses near topography of small slope: Journal of Geophysical Research, v. 86, p. 9268–9278.

Savage, W.Z., and Swolfs, H.S., 1986, Tectonic and gravitational stress in long symmetric ridges and valleys: Journal of Geophysical Research, v. 91, p. 3677–3685.

Scott, R.B., and Bonk, Jerry, 1984, Preliminary geologic map of Yucca Mountain with geologic sections, Nye County, Nevada: U.S. Geological Survey Open-File Report 84–494, 9 p., scale 1:12,000.

Springer, J.E., and Thorpe, R.K., 1981, Borehole elongation versus in situ stress orientation: Livermore, Calif., Lawrence Livermore Laboratory Report UCRL–87018, 15 p.

Stock, J.M., Healy, J.H., and Hickman, S.H., 1984, Report on televiewer log and stress measurements in core hole USW G-2, Nevada Test Site: U.S. Geological Survey Open-File Report 84–172, 31 p.

Stock, J.M., Healy, J.H., Hickman, S.H., and Zoback, M.D., 1985, Hydraulic fracturing stress measurements at Yucca Mountain, Nevada, and relationship to the regional stress field: Journal of Geophysical Research, v. 90, p. 8691–8708.

Stock, J.M., Healy, J.H., Svitek, J., and Mastin, L., 1986, Report on televiewer log and stress measurements in holes USW G-3

and Ue-25p#1, Yucca Mountain, Nevada Test Site: U.S. Geological Survey Open-File Report 86-369, 91 p.

Swolfs, H.S., and Savage, W.Z., 1985, Topography, stresses, and stability at Yucca Mountain, Nevada: paper presented at 40th U.S. Rock Mechanics Symposium, Rapid City, S.D., June 1985.

Warren, W.E., and Smith, C.W., 1985, In situ stress estimates from hydraulic fracturing and direct observation of crack orientation: Journal of Geophysical Research, v. 90, p. 6829–6839.

Zemanek, J.R., Caldwell, L., Glenn, E.E., Holcomb, S.V., Norton, L.J., and Straus, A.J.D., 1969, The borehole televiewer: A new logging concept for fracture location and other types of borehole inspection: Journal of Petroleum Technology, v. 21, p. 702–774.

Zoback, M.D., and Healy, J.H., 1984, Friction, faulting, and in-situ stress: Annales Geophysicae, v. 2, p. 689–698.

Zoback, M.L., and Zoback, M.D., 1980, State of stress in the conterminous United States: Journal of Geophysical Research, v. 85, p. 6113–6156.

Geologic and Hydrologic Investigations of a Potential Nuclear Waste Disposal Site at Yucca Mountain, Southern Nevada

U.S. GEOLOGICAL SURVEY BULLETIN 1790